Journal of Constructional Steel Research 178 (2021) 106496

Contents lists available at ScienceDirect

Journal of Constructional Steel Research

Strengthening of corroded steel CHS columns under axial compressive loads using CFRP

Omid Yousefi [a], Kambiz Narmashiri [b,*], Amir Ahmad Hedayat [c], Ali Karbakhsh [a]

[a] Department of Civil Engineering, Sirjan Branch, Islamic Azad University, Sirjan, Iran
[b] Department of Civil Engineering, Zahedan Branch, Islamic Azad University, Zahedan, Iran
[c] Department of Civil Engineering, Kerman Branch, Islamic Azad University, Kerman, Iran

ARTICLE INFO

Article history:
Received 5 June 2020
Received in revised form 18 December 2020
Accepted 21 December 2020
Available online 2 January 2021

Keywords:
Slender steel column
CFRP strengthening
Column buckling
Corrosion
Circular Hollow Section (CHS)

ABSTRACT

Stemming from unfavorable environmental conditions, corrosion can adversely affect the behavior of steel structures and damage them. To investigate this phenomenon and study the failure mode and load bearing capacity of corroded slender steel columns to retrofit them by Carbon Fiber Reinforced Polymer (CFRP), 8 equal-height slender Circular Hollow Section (CHS) column specimens were subjected to corrosive conditions at mid-height and near to bottom supports for 12, 18 and 24 hours, retrofitted by CFRP sheets and then all corroded and retrofitted columns were experimentally tested under axial compressive loading; damage dimensions were different. These specimens and two more were also studied numerically based on the Finite Element (FE) analyses of imperfected models using ABAQUS software. The specimens were first analyzed elastically to find their local and global buckling modes and then inelastically (with nonlinear geometry and material). Experimental and numerical results showed that the main problem with slender columns was their global buckling under compressive loading and corrosion reduced their load bearing capacity and ductility. According to these results, corrosion highly affected the buckling of the corroded area and deformed it axially. Regarding corroded columns retrofitted with CFRP, fibers increased the ultimate load capacity and ductility, delayed buckling of the corroded area, controlled fractures and reduced stresses in the damaged zone.

1. Introduction

Compressive members such as columns are very important components in a structure because they play a major role in bearing and transferring all the vertical and lateral loads of the building. Basically, no column can bear to its fullest capacity and fails under buckling. Depending on the application, they may fail under axial compression due to such structural instabilities as the overall/local buckling. Columns, the load bearing capacities of which are highly affected by their slenderness and length, are classified as short if $L/D < 15$ and usually fail by material crushing and local buckling, and long if $L/D \leq 15$ [1] and fail by overall buckling (L/D = slenderness ratios; L is the member length and D is its section dia.).

During the last two decades, since demand for lightweight, high performance structural systems has increased, Circular Hollow Section (CHS) steel columns have found popularity and are regularly used in the construction industry around the world. Also, they have been mostly used as the oil/gas pipeline infrastructure in the oil industry [2,3]. The structures are less likely to be capable of meeting the structural requirements for various reasons such as design and calculation problems, environmental factors, decay, and fire. The design of a cold-formed circular steel columns with different L/D ranges (maximum 50) was studied by Young et al. [4] and Huang et al. [5].

Depending on the environmental conditions, when steel members are exposed to certain substances, they are deteriorated because of many factors among which corrosion is quite serious. Corrosion is the result of repeated drying and wetting, has different intensities (Fig. 1), covers a limited area and can be quite severe in some cases because of the loss of almost the entire cross section. CHS steel columns are highly liable to corrosion and metal loss and their performance is substantially affected by the damage [8]. Corrosion reduces the metal thickness, weakens the mechanical performance and causes disastrous failure [9]. Malumbela et al. [10] studied the impacts of steel loss on the ultimate flexural load of corroded RC beams and concluded that longer drying cycles result in the highest level of corrosion.

Due to high reconstruction costs, a large portion of the countries' development budget is spent annually on the repair, rehabilitation and preservation of structures and monuments. Many researchers are interested in retrofitting them to increase their strength using new materials

* Corresponding author.
E-mail addresses: omid.yousefi88@gmail.com (O. Yousefi), narmashiri@iauzah.ac.ir (K. Narmashiri), amirahmad1356@yahoo.com (A.A. Hedayat), dr.karbakhsh@iausirjan.ac.ir (A. Karbakhsh).

https://doi.org/10.1016/j.jcsr.2020.106496
0143-974X/

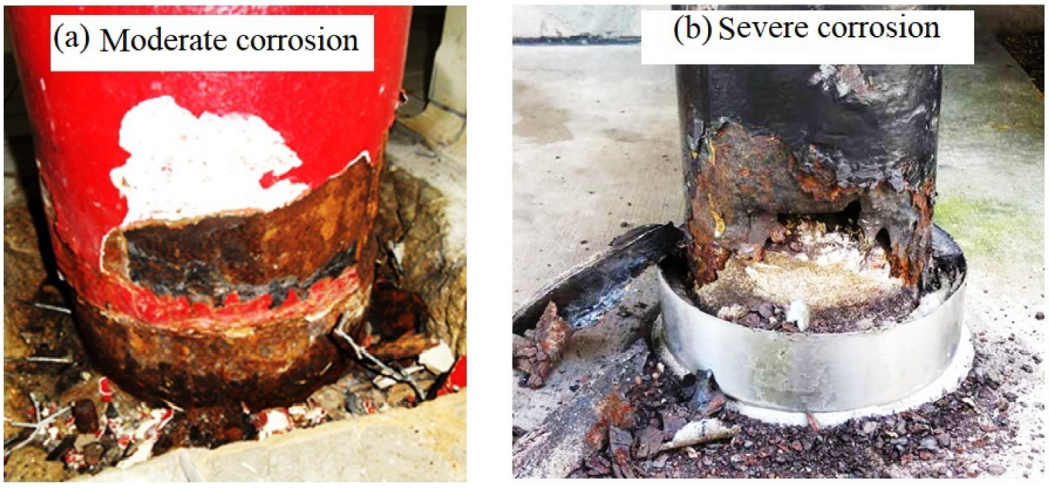

Fig. 1. Corrosion of steel columns: (a) moderate [6], (b) severe [7].

and methods. FRPs are relatively new and extensive research has been conducted on them.

Fiber effects on the strength of short columns have been studied by many researchers among which Teng et al. [11] retrofitted thin-walled circular columns (L/D = 2.7) using FRP sheets and showed that the energy absorption capacity and ductility increased and the bare specimen's failure mode under compression was outward buckling near the support (widely known as the elephant's foot collapse). In another study on short square CFRP-reinforced steel columns (with L/D = 3) under compression, Bombach and El Chalakani found out that CFRP materials could increase their strength and energy absorption capacity [12]. Bambach et al. [13] strengthened the steel SHS (with L/D = 3) using CFRP, They found out that using CFRP increases the axial capacity by up to two times and strength-to-weight ratio by one-half times. Bombach et al. [14] showed that the crushing energy and strength of short square CFRP-reinforced steel columns with L/D = 3, depended on the type of steel and the width-to-thickness ratio of the CFRP, and concluded that using fibers increased the columns' ultimate bearing capacity. Also, the failure mode for both static and dynamic loads was axial crushing.

Haider and Zhao [15] retrofitted short columns (with L/D in the 2.7–3.2 range) with CFRP fibers transversely and longitudinally and observed that the fiber direction affected the yielding capacity and the onset of buckling. Besides, local failure in the form of outward buckle near the support emerged and for samples with less thickness, buckling occurred in the middle of the column.

In general, the common failure of long columns is due to overall buckling, which affects the column's structural parameters. Mirmiran et al. [16] studied the effects of L/D = 2.1 to 18.6 on the behavior of the concrete-filled FRP tubes and found that an increase in the slenderness: 1) reduced the column strength and 2) caused the failure not to precisely occur at the mid-height because it was affected by the load eccentricity, column alignment or the curvature developed along the column. Pan et al. [17] studied the slenderness effects on the behavior of FRP-wrapped RC columns (L/D in the 3.3–20 range) and showed that an increase in the column slenderness significantly reduced the retrofitting effects. Karimi et al. [18] studied the effects of the slenderness on the behavior of steel-concrete composite columns by testing a total of nine columns (L/D ranging from 3.3 to 20) and found that the FRP jacket increased the concrete compressive strength up to 17%. Long composite column specimens indicated high stability against global buckling and, consequently, enhanced the buckling capacity of long steel columns.

Using the appropriate technique has a significant impact on the retrofitting, Silvestre et al. [19] studied the nonlinear behavior and load bearing capacity of cold-formed lipped channel steel columns (with L/D in the 5.9–21.5range). They compared short and long columns and studied the effects of different strengthening techniques. Fibers were used longitudinally and transversely and results showed that the transverse strengthening of long columns' outer surface increased the ultimate load bearing capacity by about 20%, while for short ones, longitudinal wrapping was more effective.

Not only the buckling, but also the resulting damage affects the column's structural performance. Karimian et al. [20] studied the effects of the vertical and horizontal defects artificially created on short circular steel columns (L/D = 1.5) strengthened with CFRP and showed that the bearing capacity was reduced while the axial deformation and local buckling were increased. An increase in the load increased the stress in the damaged area around the defect causing a local, symmetrical and outward buckling on both sides of the defect.

Ghaemdoust et al. [21] studied short square (L/D = 3) damaged steel columns having horizontal and vertical defects at the corner and center of the column and showed that there was inward local buckling for the vertical defect while for the horizontal one, the local buckling was outward.

Earlier studies have shown that using CFRP for column retrofitting highly improved the column strength and ductility; however, more investigations are needed to develop the CFRP sheets application to confine corroded long steel columns under axial loads. This study is aimed to first evaluate the compressive behavior of long steel CHS columns (L/D = 34) with artificial corrosion, while major existing researches are on short and medium-length columns. Then, employ the FRP strengthening technique to cover the corroded area because corrosion destroys the steel surface and directly affects the ultimate load bearing capacity, ductility, and energy dissipation; retrofitting methods can also be used to strengthen the existing steel columns, piles, and bridge piers. In this paper, defective slender columns were prepared with and without CFRP strengthening and subjected to three corrosion grades at two different locations, and effects of such parameters as the dimension, defect severity and CFRP wrapping on their behavior were investigated both experimentally and numerically.

2. The research study

2.1. The experiments

To study the effects of corrosion and strengthening techniques on the behavior of corroded columns, this research did experimental tests on eight slender steel column specimens among which one was without

damage for controlling purposes. The specimens were subjected to corrosion at their mid-height or close to the supports for 12, 18 and 24 hours.

2.1.1. Characteristics of the selected CHS steel column

The geometrical and material properties of the selected steel column obtained from the experimental coupon test (ASTM A370-17a [22]) are listed in Table 1 where D, t and L are the column's outer diameter, wall thickness and length and E, f_y, f_u and ε are the elasticity modulus, yield stress, ultimate stress and percent elongation of the steel material, respectively. Three tensile test were performed, and the mean values are presented in Table 1. The tensile test, the failure mechanism, and its experimental stress-strain curve are shown in Figs. 2 and 3, respectively. The steel CHS specimens were manufactured as Grade SPHT3 conforming to JIS G 3132 [23].

2.1.2. CFRP

This study has used four CFRP layers (SikaWrap®-230C) (Table 2) with elasticity modulus, Poisson ratio and thickness equal to 238,000 MPa, 0.12 and 0.131 mm, respectively to strengthen the corroded columns. Fibers are unidirectional having a linear elastic stress-strain relationship up to the rupture. Authors did some primary modeling to select the CFRP type (as they did in their previous researches [20 and 21]) and showed that the higher was the elasticity modulus the more were the positive effects on the retrofitting of damaged steel columns.

2.1.3. Adhesive

The Sikadur®-330 epoxy adhesive (Table 2) used in this study is recommended by the CFRP producer and has an elasticity modulus and tensile strength equal to 4500 and 30 MPa, respectively. It is commonly used for SikaWrap®-230C CFRP where the mixing ratio of the resin and harder parts is 1:4.

2.1.4. The specimens

Out of the eight test columns (Table 3), two were externally wrapped with 200 mm-long CFRP sheets and the remaining six were un-bonded (five with corrosion and one undamaged for controlling purposes) (Figs. 4 and 5). Out of the four CFRP layers used for strengthening, the first and the third are placed transversely and the second and the fourth are attached longitudinally (Fig. 6). The corrosion-free non-strengthened control column is used for the comparison of the load bearing capacity and ductility of other specimens. In this study, MD is the mid-height damage, SD is near-the-support damage, corrosion rates correspond to 12H, 18H and 24H and 2T2L is the strengthened column (e.g., MD-18H-2T2L means a strengthened slender column where the 18 hr-corrosion damage occurs at the mid-height).

2.1.5. Corrosion setup

An 80 mm diameter plastic pipe was attached to the steel circular columns due to applying corrosion to the mid-height or at a distance 50 mm from the edge of the support (Fig. 7), and the process continued for 12, 18 and 24 hours. A 12-v, 30-amp, regulated DC power supply transmitted a constant 5-amp current to each phase wire by putting a resistor in its path, and the current was applied to four 5-mm thick rods installed with a weak weld at the same distance from the center of the damage to create a constant phase current for uniform damage around the desired area. The zero wire was attached to a stainless screw inside a 5% sodium chloride solution (Fig. 7), the percent concentration of which was adopted from Malumbela et al. [10]. Within 12 hours, the thickness of the corroded area was reduced by 1 mm making a small hole in the specimen and in 18 hours, the damaged area was utterly destroyed; the maximum horizontal length of near-the-support damage was 64.1 mm and that of the mid-height damage was 63.8 mm. In specimens with 24-hour corrosion, an 80 mm-diameter, fully damaged, circular area was created at the defected location (Fig. 8).

To achieve a good column-fiber bond, the specimens were sand blasted on the outer surface to eliminate the corrosion, then acetone was used to clean all the contamination from the steel and CFRP surfaces and, finally, CFRP sheets were wrapped around the specimens (Fig. 9) and kept at room temperature for seven days (as the fiber manufacturer had recommended).

2.1.6. Experimental setup

To measure the deformations, three LVDTs (Linear Variable Differential Transformer) were installed, one under the hydraulic jack and two around the mid-height. Corroded columns experienced global buckling in various directions with different angles under compressive loads, and since horizontal displacements had different values, all columns were compared based on axial shortening. To study the corrosion effects, pin-ended boundary conditions were chosen to allow column to buckle in any direction, and to store the corresponding data, the load cell and LVDTs were connected with a 16-Channel data logger system. The test setup of the specimens is shown in Fig. 10.

Specimens, with 10 mm-thick, 30 mm-high caps welded at both ends to thick steel plates to ensure uniform loading over the entire cross section, underwent axial loading, underwent axial loading.

Table 1
Sizes and properties of the CHS steel column.

D (mm)	t (mm)	L (mm)	E (MPa)	f_y (MPa)	f_u (MPa)	Elongation (ε) %
88	2.06	3000	216,000	261	322	10.7

Fig. 2. Tensile test and the failure mechanism.

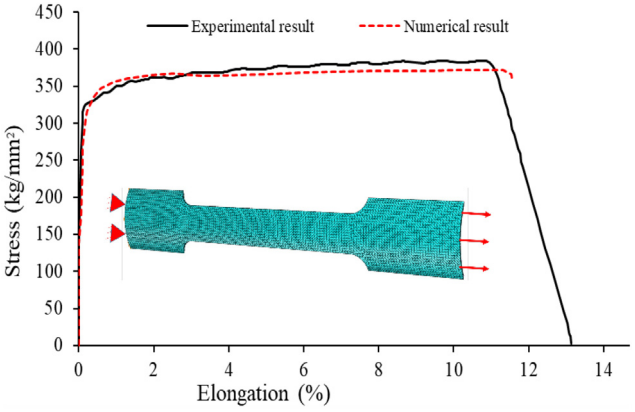

Fig. 3. Stress-strain curve for the steel material.

Table 2
CFRP and adhesive specifications.

Material	Thickness (mm)	Tensile strength (MPa)	Modulus of elasticity(MPa)	Ultimate strain (%)
CFRP (SikaWrap_-230 C) [24]	0.131	4300	238,000	1.8
Adhesive (Sikadur_-330) [25]	0.869	30	4500	0.9

According to Figs. 11 and 12, there is a small gap between the column and end caps to settle the specimen on its supports easily, correctly and concentrically through guide line provided on the end plates; then, the loading started gradually. Each column was then tested under axial compressive load and its deformation and load carrying capacity were recorded accurately.

2.2. The numerical analyses

A total of 10 specimens were studied numerically (Table 3); three were strengthened with CFRP sheets, six were un-bonded and defective and one was un-bonded and undamaged (for controlling purposes). The applied damage depended on the extent of corrosion on the lab specimen; for a 12-hr corroded column, since the thickness was reduced by 1 mm, the same reduction was applied to the model, but in 18- and 24-hr cases, the created cut was equal, in area, to the corroded part of the test specimen. It is noteworthy that eight columns were studied experimentally and numerically and two more were simulated by FE modeling to investigate the effects of the fiber length and 24-hour corrosion in the mid-column. Numerical views of non-strengthened CHS steel section are shown in Fig. 13.

2.2.1. General

A non-linear finite element model (FEM) has been developed using ABAQUS V 6.16 to simulate the buckling behavior of ten corroded CHS steel sections strengthened with CFRP sheets considering the geometry, material properties, and the initial local and global geometric imperfections as the modeling parameters.

2.2.2. Type of element and material modeling

A ten-nodded solid element (C3D10R) with reduced integration was used to study the structural behavior and Von-Mises stresses along the CHS thickness, especially in the damaged zone; the mesh size was 12 mm and the materials properties were assumed to be nonlinear in the FE analyses. CFRP sheets and adhesive were simulated using 3D-20-node HEX element (C3D20R) and 5 mm mesh size and Tie method was used to connect the adhesive and CFRP to the CHS steel column to generate the desired surface interaction. CFRP fibers were defined as linear and orthotropic in the software because of their linear and unidirectional properties and adhesive properties were defined linearly. Since each CFRP longitudinal/transverse layer was modeled with different parts to consider its orientation, and the in-plane shear strength was quite less than the normal tensile strength, use was made of the laminar behavior with a small shear modulus.

2.2.3. Boundary conditions and analysis types

To enable meaningful numerical-experimental results comparisons, an adequate simulation of the member end boundary conditions is a necessity. Based on the laboratory setup, all translational DOFs were restrained at both column ends, except for the displacement at the loaded end in the direction of the applied load; other nodes were free to translate and rotate in any direction. The boundary conditions were modeled by two reference points one at each column end at the center of the cross section connected to the nodes of two ends by two rigid body constraints. Due to the axial displacement, the load was applied to the reference point at the loading edge (similar to the lab specimen tests).

Since the Riks method is generally employed to predict a structure's unstable, geometrically nonlinear break fall that consists of nonlinear materials/boundary conditions, it was used in this study to perform nonlinear analyses to accurately obtain the failure modes and post buckling behavior; to this end, imperfect models were used for the analyses under monotonic loadings. Imperfection components are generally local and global; the latter was measured, prior to testing, by a theodolite at the mid-length (δ) over the column length (L) along the weld of all specimens; the mean value of these measurements was approximately L/1200 for all the specimens. To create the imperfect model in this research, the buckling mode shapes were first computed in separate analyses and then the first two modes, with imperfection values of L/1200 (global) and 5% of the column wall thickness (local), were combined. Since the maximum local imperfection is generally unknown, it can be obtained by trial and error to bring the numerical and experimental results closer as regards 1) the load-displacement relationship and 2) the deformed shape of the specimen; in [26,27], this value was either 1% or 5% of the plate thickness apt to buckling during loading.

2.2.4. Validation of the numerical models

In the FE analyses, since materials were assumed to have nonlinear properties their behavior was first verified based on the experimental stress-strain curve obtained from the coupon test. Fig. 3 compares the numerical and experimental coupon test results and shows that they

Table 3
Specifications, damage dimensions and load bearing capacities of the specimens.

No	Specimen	Corrosion			CFRP length (mm)	E_d (kN.mm)	Ductility index (DI)	Load bearing Capacity			
								Experimental		Numerical	
		Time (Hrs.)	Percentage (%)	Position				Load (kN)	Increase/ decrease (%)	Load (kN)	Increase/ decrease (%)
1	Control	N/A	N/A	N/A	N/A	386	1.31	132.02	–	130.1	–
2	MD-12H	12	50	Middle	N/A	301	1.24	113.9	−13.7	114	−12.3
3	MD-18H	18	100	Middle	N/A	266	1.17	78.2	−40.7	80.01	−38.5
4	MD-18H-2T2L	18	100	Middle	200	380	1.30	123.04	−6.8	120	−7.7
5	MD-18H-2T2L400	18	100	Middle	400	413	1.33	N/A	N/A	138.9	+6.7
6	MD-24H	24	100	Middle	N/A	132	1.15	N/A	N/A	65.05	−50
7	SD-12H	12	50	Near the support	N/A	381	1.30	123.5	−6.4	122	−6.22
8	SD-18H	18	100	Near the support	N/A	372	1.28	103.4	−21.67	104	−20
9	SD-18H-2T2L	18	100	Near the support	200	376	1.46	127.1	−3.8	125.1	−3.81
10	SD-24H	24	100	Near the support	N/A	370	1.265	84.198	−36.2	85.35	−34.4

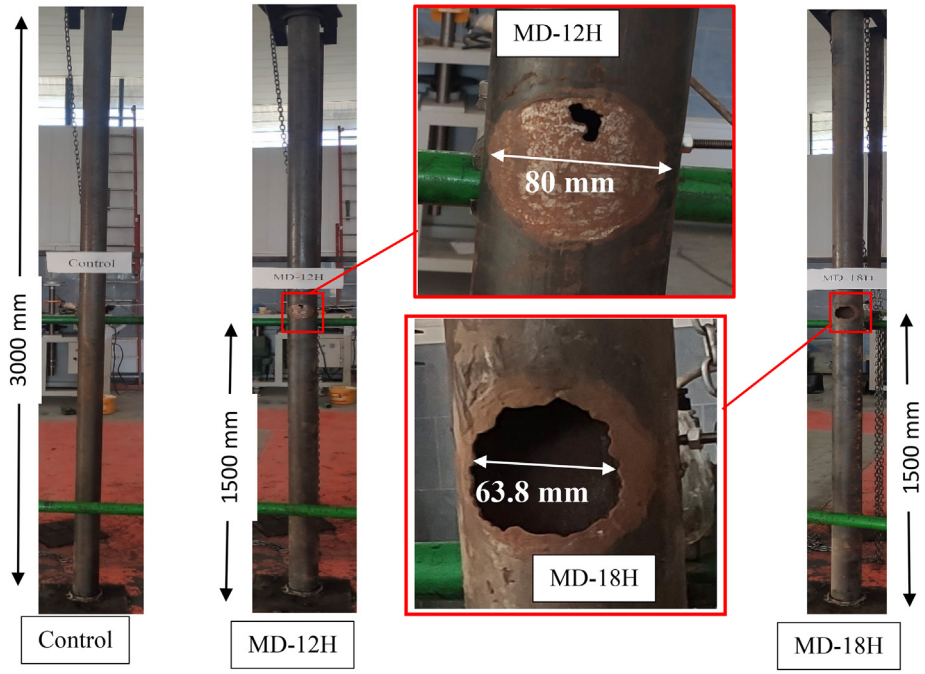

Fig. 4. Experimental views of non-strengthened control column and specimens with mid-height corrosion.

agree well. Then, the experimental results of the MD-18H-2T2L and control specimens were compared to the analytical results (obtained from FE models) through their load-displacement curves and deformations to verify the model accuracy (Figs. 14 and 15). As shown, the comparisons show good agreement which is an indication of the FE modeling accuracy.

3. Results and discussion

Since each structural member should have enough strength, stiffness, and ductility, and defects usually affect all, proper confinement techniques are quite vital to improve them, especially in earthquake-prone areas. As the ductile behavior during a vertical collapse gives a noticeable warning regarding the onset of the column failure and provides enough time for a safe building evacuation, this study addressed it using the ductility index and energy dissipation capacity parameters. These plus the load bearing capacity and failure modes will be discussed in details in the following sections.

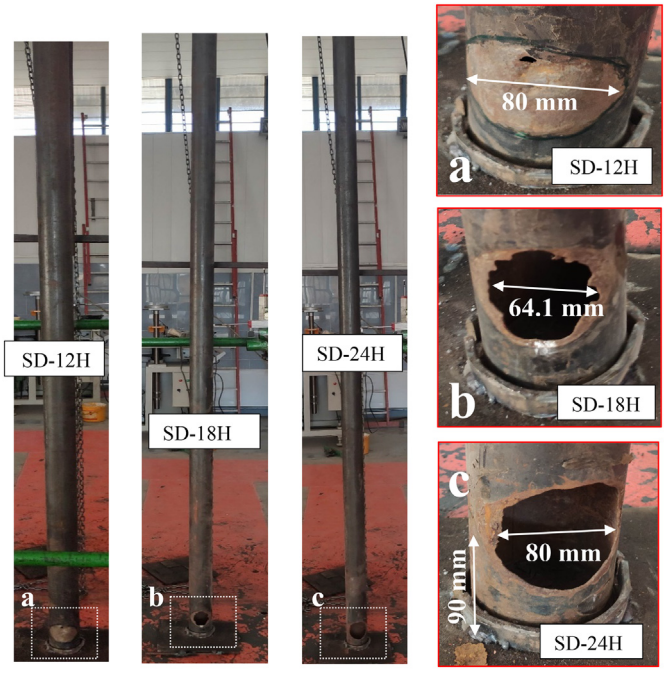

Fig. 5. Experimental views of non-strengthened CHS steel section with near-the-support corrosion.

3.1. Failure modes

In the present research, the experimental and numerical analyses of slender circular columns were carried out under axial compressive loading which continued until the ultimate load and plastic strain occurred. Under high compressive stresses, slender columns tend to buckle along

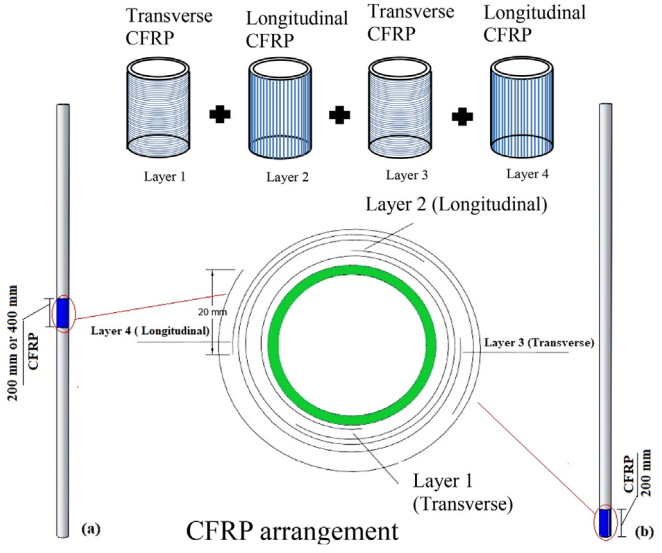

Fig. 6. CFRP location and arrangement.

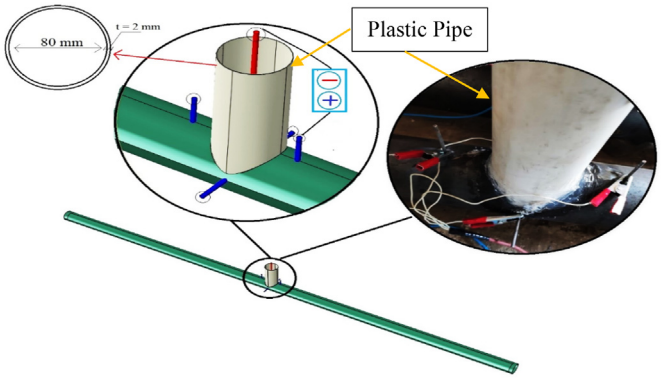

Fig. 7. Experimental corrosion setup.

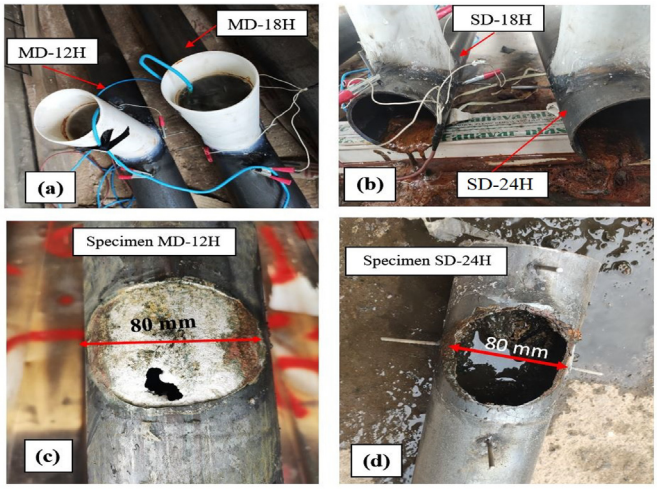

Fig. 8. Specimens under and after the corrosion process: (a) specimens MD-12H and MD-18H, (b) specimens SD-18H and SD-24H, (c) specimen MD-12H, (d) specimen SD-24H.

the column height (have global buckling) before reaching the ultimate load, but short columns tend to experience local buckling.

The initial failure in the control column was global buckling with significant mid-height local deformations; as loading continued to enter the plastic area, the column experienced a mid-height local buckling and a secondary failure (Fig. 14).

In MD-12H, the stress increase in the mid-height and vicinity of the corrosion zone resulted in a local buckling, after the global buckling, observed as crumples (Fig. 16) because of the reduced thickness and stiffness.

In MD-18H, an increase in corrosion increases the damaged area causing failure to occur more quickly; hence, outward buckling on both sides of the defect will reduce the width of the corroded area. It is noteworthy that all columns with mid-height damage experience global buckling and they bend in the direction of the damage zone (Fig. 17).

Damaged columns showed better structural performance at the base and bore compressive loads better. Since the damage area thickness reduced, SD-12H failure occurred and local buckling was visible. Both SD-18H and SD-24H experienced outward buckling on both sides of the corroded area with their global buckling tending to bend in a direction opposite to the damage side (Fig. 18).

For the confined specimens, the CFRP ruptured at the corroded columns. In SD-18H-2T2L and MD-18H-2T2L strengthened using 200 mm-long CFRP, compressive loading intensified the stress in CFRP fibers leading, to a shear rupture. Then, local buckling occurred around the corroded zone. Fibers reduced the column stresses significantly and delayed the local buckling. Figs. 19 and 20 show CFRP rapture failure on the damage area.

The numerical results show that the global buckling occurred along the column and lead to increase in Von-Mises stresses at corroded area which resulted in local buckling. To study the effects of the fiber length and 24-hr mid-column corrosion, MD-24H and MD-18H-2T2L (strengthened with 400 mm-long CFRP) were simulated by FE modeling. The former had outward buckling on both sides of the damaged area, and the latter, with longer retrofitting compared to 200 mm-CFRP, experienced reduced stress intensity at the defect area (Fig. 21). In numerical cases, buckling occurred in the damaged area and stress intensity was clearly visible around it. In overall buckling of the middle-

Fig. 9. Preparing CFRP-strengthened specimens.

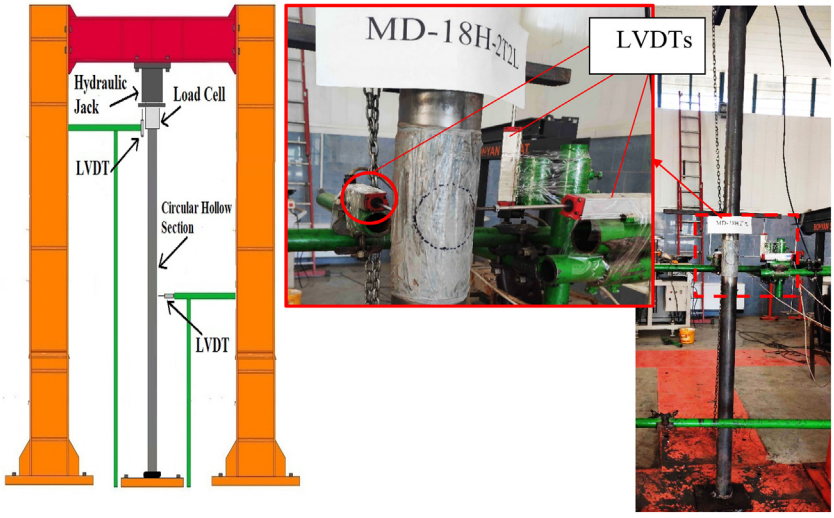

Fig. 10. Columns under hydraulic jack and installation of LVDTs.

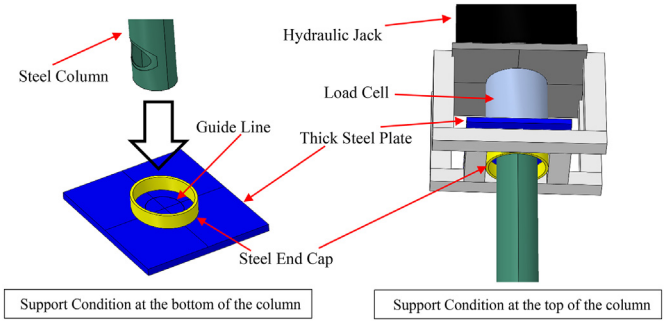

Fig. 11. Technique of capping the long column ends.

damaged specimens, they bended in a direction of located damage, while it was reverse for corrosion near the supports.

3.2. Load carrying capacity

Load-Axial shortening curves of the 8 tested specimens are shown in Figs. 22, 23, and 24, and their details plus their maximum load bearing capacity are presented in Table 3. To study the corrosion effects on two column areas (mid-height and near the support), they were subjected to 12-, 18- and 24-hr corrosion; after 12 hours, the corroded area lost 1 mm of its thickness resulting in a load bearing capacity reduction of 13.7 and 6.4% due to the mid-height and near-the-support damage, respectively. After 18 hours, the corroded area surface (with a maximum horizontal length of about 64 mm) was totally destroyed; the ultimate load reduction for the mid-height damage was 40% and for near-the-support damage was 21%. After 24 hours, the damaged area was maximum 80 mm long at the column base and the load bearing capacity was 84.198 kN (7% more than 78.2 kN for 18-hr mid-height corrosion) concluding that the latter has a more destructive effect on the load carrying capacity than near-the-support case. Since the ultimate mid-height load bearing capacity reduction can be due to the global and local buckling concentration in the same area, and corrosion affects the area and modulus of cross-section forcing the center of gravity to move, a further local eccentricity is created, besides weakening the cross-section, that causes the column to perform under the combined effects of both of them. As moment is significantly lower near the support, the damage has less effect on the load bearing capacity in this area.

To compensate for this reduction, 200-mm long CFRP sheets (2 transverse and 2 longitudinal layers) was employed which increased

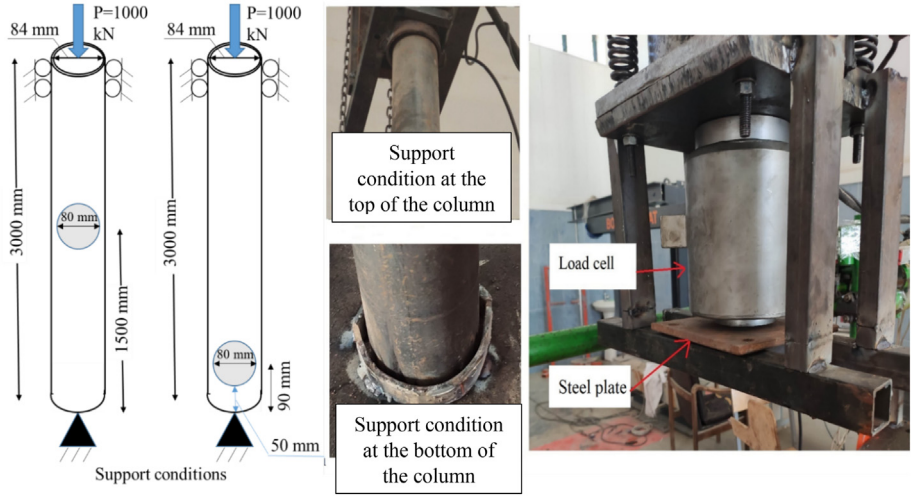

Fig. 12. Columns specifications and boundary conditions.

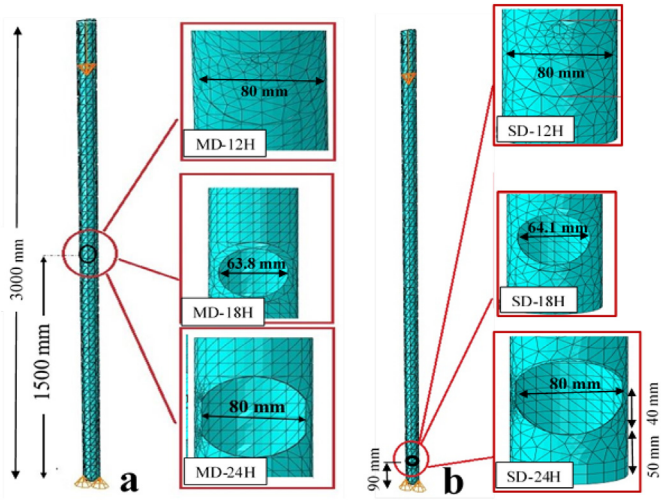

Fig. 13. Numerical views of non-strengthened CHS steel section: (a) mid-height corrosion, (b) near-the-support corrosion.

the load bearing capacity by 33.9% compared to the non-strengthened corroded specimen. The 200-mm long sheet was also used to strengthen the SD-18H case resulting in an ultimate load increase of 47.4%, which means the fibers have performed well when wrapped around the damaged steel columns. Fig. 24 compares the load-displacement curves of specimens with mid-height damage and those with near-the-support damage. As shown, the former show lower strength and experience a sudden failure after buckling.

Comparing the experimental and numerical results of the load bearing capacity (Table 3) proved that they were close and had good accuracy; for the control column, the ultimate numerical load was 130 kN, indicating only 2% error compared to the experimental value. In MD-24H, the ultimate load was 65.05 kN (reduced by 50% compared to the control column) confirming that the mid-height corrosion effect was more than that near the support with equal damage area. Using 400 mm-long CFRP fibers to confine MD-18H-2T2L increased the ultimate load by 45.2% (12% more than that by 200 mm-long ones).

Fig. 14. Experimental and FE failure modes for the plain specimen.

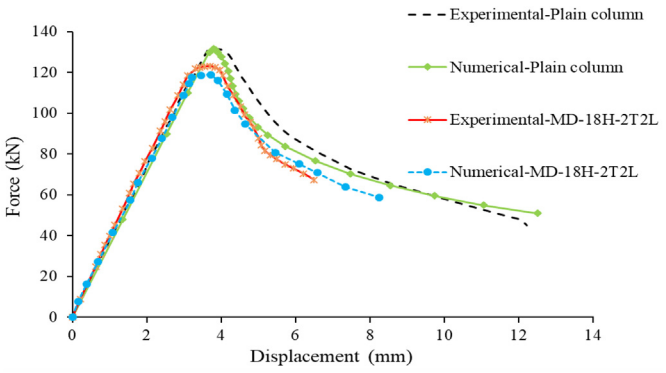

Fig. 15. Load- vertical displacement curves validation of plain column and strengthened specimen MD-18H-2T2L.

3.3. Ductility index

Since columns should undergo large vertical-collapse deformations without failing and corrosion can prevent this, studying the ductility and energy dissipation capacity of corroded columns and using proper retrofitting methods are of great importance. The ductility index (DI) and the columns' energy dissipation capacity (E_d) were evaluated (Similar to [18],) using Eqs. (1) and (2), respectively.

$$DI = \frac{\delta_{85\%}}{\delta_y} \tag{1}$$

$$E_d - \frac{1}{2} P_u . \delta_y + P_u (\delta_u - \delta_y) \tag{2}$$

where $\delta_{85\%}$ is the axial displacement corresponding to 85% of the ultimate load (P_u) (Fig. 25), $\delta_y = \delta_{75\%}/0.75$. $\delta_{75\%}$ is the axial displacement corresponding to the 75% ultimate load in the pre-peak stage (Fig. 25) and δ_u is the axial displacement corresponding to the ultimate load. To predict the energy dissipation capacity (E_d) [18], use was made of the area under the load-displacement curve until break down.

It seems that Eqs. (1) and (2) assess the structural elements' ductile behavior after and before reaching the ultimate load, respectively, with a dropping rate depending directly on the column ductility, especially under gravity loads. After the peak load, long columns experience a sudden strength loss with a rate relatively faster in corroded columns maybe due to a deflection preventable by an effective strengthening

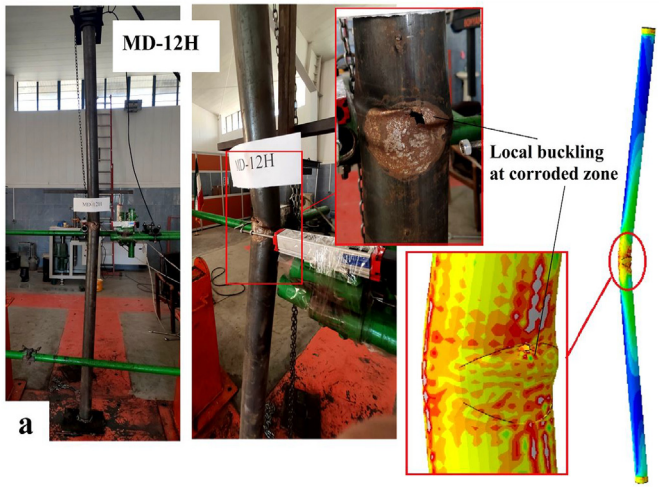

Fig. 16. Failure modes in MD-12H.

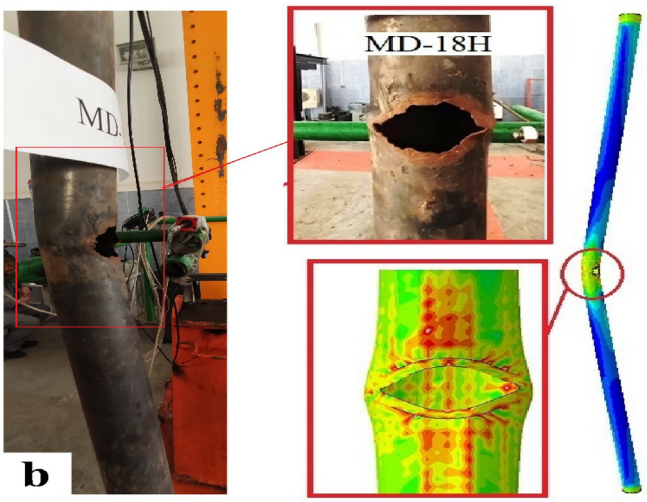

Fig. 17. Failure modes in MD-18H.

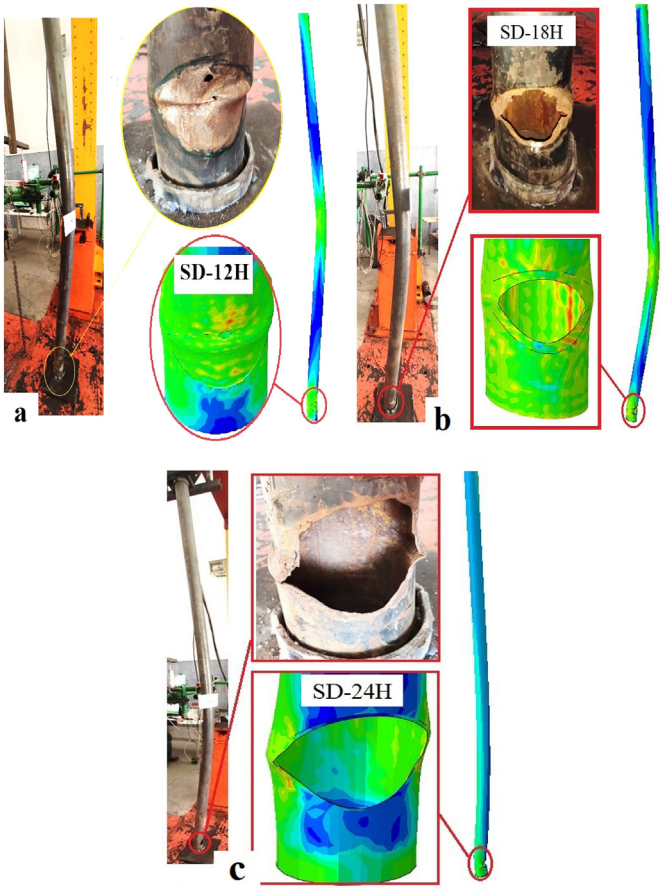

Fig. 18. Comparison of the specimens' failure modes: (a) SD-12H, (b) SD-18H, (c) SD-24H.

method. On the other hand, the ductility index can show the rate of the load drop and reveal effectiveness of the corrosion and retrofitting method by comparing the obtained values.

The DI and E_d values for all specimens are summarized in Table 3; as shown, since DI is 1.31for the bare column and 1.265 for SD-24H, (small difference) effect of the near-the-support corrosion is negligible, but the mid-height corrosion reduces the DIs of MD-18H and MD-24H about 12%. CFRP wrappings increase the column ductility with mid-height

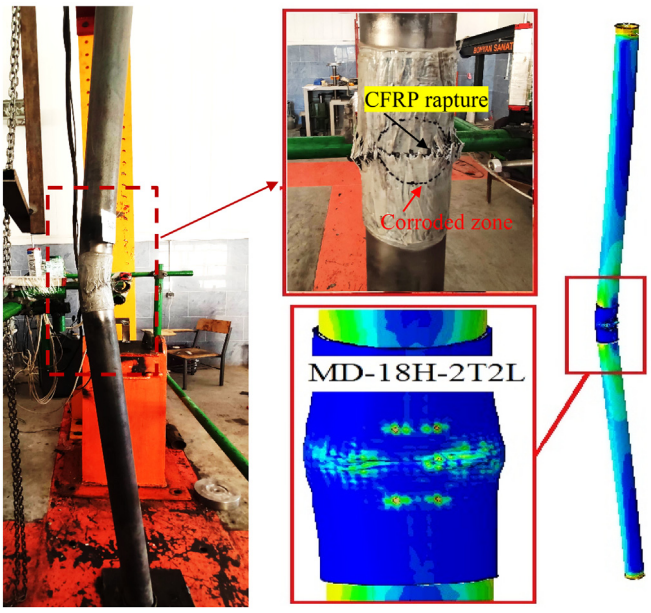

Fig. 19. CFRP failure modes in MD-18H-2T2L with 200 mm CFRP length.

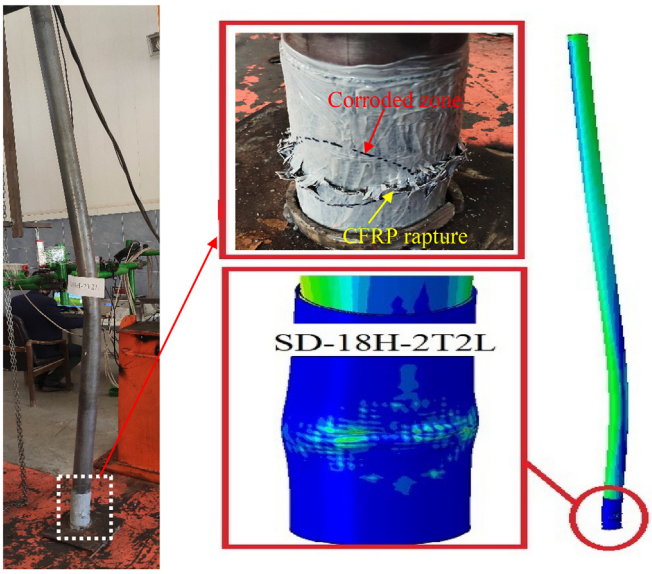

Fig. 20. CFRP failure modes in SD-18H-2T2L.

damage because they have high elasticity modulus; using 400-mm long CFRP in MD-18H-2T2L increased the ductility by 2% compared to the control specimen.

Eq. (2) that computes energy dissipation, can be used to examine the ductile behavior before reaching the ultimate load (the area under the load-displacement curve; peak load and yield point) and provide criterion for strain hardening of corroded columns; the larger the energy dissipation, the greater the amount of strain hardening.

Compared to the control column (with 386 kN.mm energy dissipation capacity), cases with near-the-support damage (SD-18H and SD-24H) showed a reduction up to 4%, mid-height damage reduced this capacity substantially, and MD-18H and MD-24H experienced 32% and 65% reduction, respectively, indicating that the mid-height damage is more critical compared to near-the-support damage. For case MD-18H-2T2L confined by 200 and 400 mm CFRP sheets, a capacity gain of 42 and 55%, in comparison with specimen MD-18H was observed

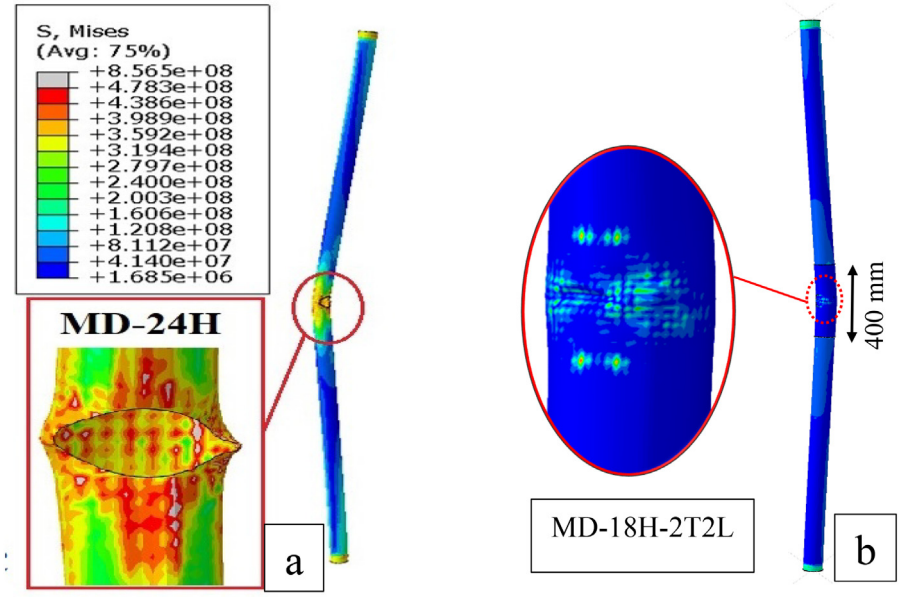

Fig. 21. Failure modes: (a) MD-24H, (b) MD-18H-2T2L with 400 mm CFRP length.

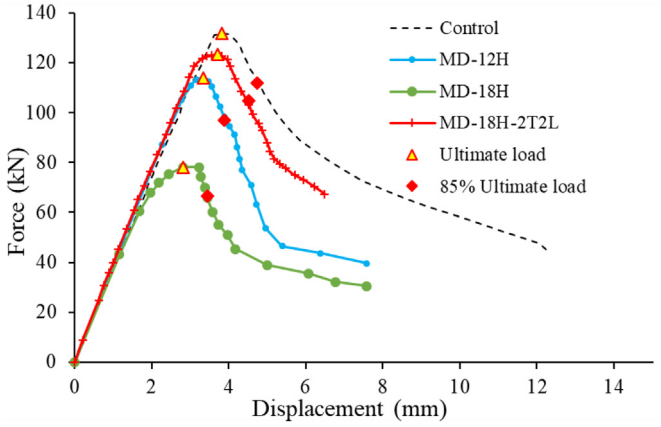

Fig. 22. Experimental load-deflection (vertical) of columns with mid-height damage compared to the control specimen.

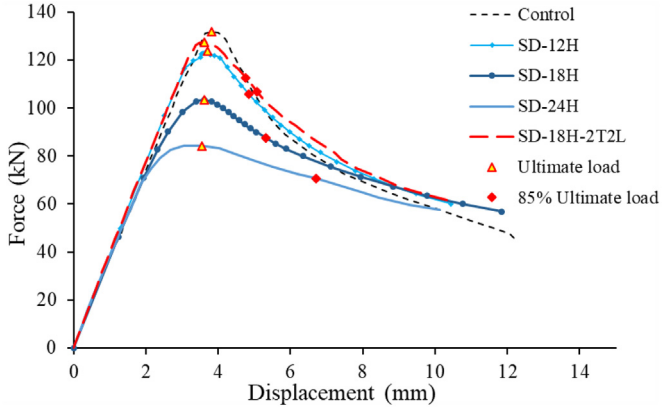

Fig. 23. Experimental load-deflection (vertical) of columns with near-the-support damage compared to the control specimen.

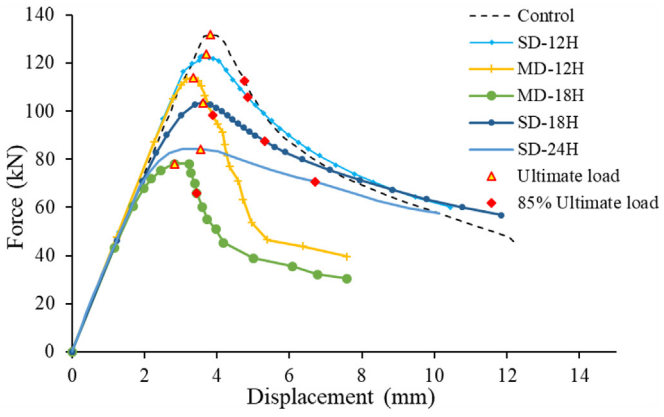

Fig. 24. Experimental load-deflection (vertical) of columns with mid-height damage compared to near-the-support damage.

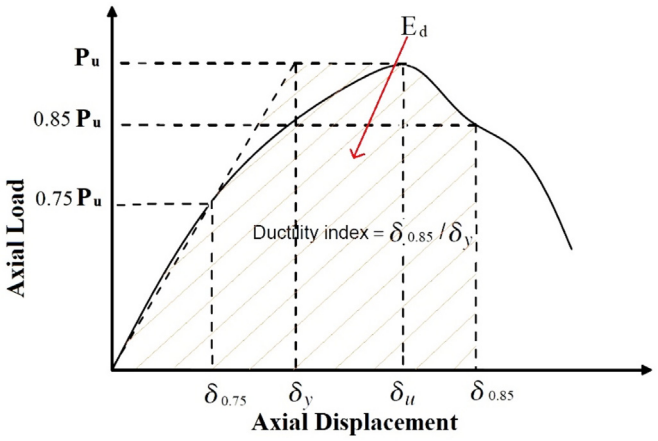

Fig. 25. Definition of ductility index and energy dissipation capacity [18].

respectively. CFRP strengthening methods have shown that they can appropriately compensate for the lost energy dissipation capacity. The specimens' evaluated ductility indexes and energy dissipation capacities are presented in Table 3.

4. Conclusions

This study investigated, experimentally, the behavior of corroded slender steel columns with and without strengthening under compressive axial loading considering their buckling and corrosion. Corroded columns were strengthened with CFRP sheets and corrosion was applied to the column mid-height and near the supports for 12, 18, and 24 hours. In addition to experimental tests, these circular columns were also studied numerically based on FE modeling where the buckling analyses were first performed to obtain the buckling modes to create imperfected models and then nonlinear Riks analyses were used to achieve the post-buckling failure. Since dynamic loads have major effects on corroded members' behavior, selecting different corrosion locations and area sizes on long circular steel columns under the fatigue load can be a topic for further future studies.

The research was aimed to investigate the effects of damage on the columns' load bearing capacity and retrofitting damaged zones to compensate for the strength loss of circular slender steel columns. To this end, ten columns with different defects were compared and the following results were obtained:

Columns with mid-height defects experienced significantly lower load bearing capacity than those having corrosion at their supports. Results concluded that a reason for this greater reduction can be the concentration of the column's global and local buckling in the same area. Also, both the area and the modulus of the cross-section are affected by the damage, which causes the center of gravity to move and resulting in less moment for the defects close to the base. As the level of corrosion increased, the stress intensity increased in the defected area causing the ultimate load to reduce more noticeably. Long columns experienced a sudden drop in strength after passing the elastic zone due to their instability and presence of damage, especially where the global buckling was the highest; this affected the structural performance of the corroded columns considerably. Regarding the energy dissipation capacity, corrosion played the leading role and reduced it by up to 65%; this was substantial for columns with mid-height damage compared to those with near-the-support damage. A sudden decrease in strength reduced the column stability under monotonic loads and shortened the time of the final failure. The ductility index study for corroded columns indicated that an increase in the corrosion time increased strength loss abruptly, which is a logical justification of the reduced ductility of steel columns.

For all strengthened specimens, retrofitting with externally bonded CFRP fibers under compressive loads increased the ductility compared with the unwrapped ones. CFRP strengthening postponed the local buckling and reduced the stress intensity in the damage location. In confined specimens, stresses were concentrated around the damaged area leading, finally, to a rupture failure due to the continued loading.

Declaration of Competing Interest

The authors declare that they have no known competing financial interests or personal relationships that could have appeared to influence the work reported in this paper.

Acknowledgements

The authors are indebted and would like to express their gratitude to the Islamic Azad University, Sirjan & Zahedan Branches, Sirjan & Zahedan, Iran, for their appreciable supports for the study presented here.

References

[1] British Standards Institution, British Standard for Structural Use of Concrete, London, BS 1997 8110.
[2] J.A. Beavers, N.G. Thompson, External corrosion of oil and natural gas pipelines, ASM HandBook, 13, 2006, pp. 1015–1025.
[3] J. Wardenier, J. Packer, X. Zhao, G. Van der Vegte, Hollow Sections in Structural Applications, Bouwen met staal Rotterdam, The Netherlands, 2002.
[4] B. Young, W. Hartono, Compression Tests of Stainless Steel Tubular Members, 128 (6), 2002 754–761.
[5] Y. Huang, B. Young, Design of cold-formed stainless steel circular hollow section columns using direct strength method, Eng. Struct. 163 (2018) 177–183.
[6] www.stressuk.co/wp-content/uploads/2014/09/1_Carbon_Langley.png.
[7] www.constructionspecifier.com/wp-content/uploads/2018/04/Photo-2-comp-500x375.jpg.
[8] M. Elchalakani, Rehabilitation of corroded steel CHS under combined bending and bearing using CFRP, J. Constr. Steel Res. 125 (2016) 26–42.
[9] A. Cinitha, P. Umesha, N.R. Iyer, An overview of corrosion and experimental studies on corroded mild steel compression members, KSCE J. Civ. Eng. 18 (6) (2014) 1735–1744.
[10] G. Malumbela, M. Alexander, P. Moyo, Variation of steel loss and its effect on the ultimate flexural capacity of RC beams corroded and repaired under load, Constr. Build. Mater. 24 (6) (2010) 1051–1059.
[11] J. Teng, Y. Hu, Behaviour of FRP-jacketed circular steel tubes and cylindrical shells under axial compression, Constr. Build. Mater. 21 (4) (2007) 827–838.
[12] M.R. Bambach, M. Elchalakani, Plastic mechanism analysis of steel SHS strengthened with CFRP under large axial deformation, Thin-Walled Struct. 45 (2) (2007) 159–170.
[13] M.R. Bambach, H.H. Jama, M. Elchalakani, Axial capacity and design of thin-walled steel SHS strengthened with CFRP, Thin-Walled Struct. 47 (10) (2009) 1112–1121.
[14] M.R. Bambach, H.H. Jama, M. Elchalakani, Static and dynamic axial crushing of spot-welded thin-walled composite steel–CFRP square tubes, Int. J. Impact Eng. 36 (9) (2009) 1083–1094.
[15] J. Haedir, X.-L. Zhao, Design of short CFRP-reinforced steel tubular columns, J. Constr. Steel Res. 67 (3) (2011) 497–509.
[16] A. Mirmiran, M. Shahawy, T. Beitleman, Slenderness Limit for Hybrid FRP-Concrete Columns, 5(1), 2001 26–34.
[17] J.L. Pan, T. Xu, Z.J. Hu, Experimental investigation of load carrying capacity of the slender reinforced concrete columns wrapped with FRP, Constr. Build. Mater. 21 (11) (2007) 1991–1996.
[18] K. Karimi, W.W. El-Dakhakhni, M.J. Tait, Behavior of slender steel-concrete composite columns wrapped with FRP jackets, J. Perform. Constr. Facil. 26 (5) (2012) 590–599.
[19] N. Silvestre, B. Young, D. Camotim, Non-linear behaviour and load-carrying capacity of CFRP-strengthened lipped channel steel columns, Eng. Struct. 30 (10) (2008) 2613–2630.
[20] M. Karimian, K. Narmashiri, M. Shahraki, O. Yousefi, Structural behaviors of deficient steel CHS short columns strengthened using CFRP, J. Constr. Steel Res. 138 (2017) 555–564.
[21] M.R. Ghaemdoust, K. Narmashiri, O. Yousefi, Structural behaviors of deficient steel SHS short columns strengthened using CFRP, Constr. Build. Mater. 126 (2016) 1002–1011.
[22] ASTM, ASTM A370-17a: Standard Test Methods and Definitions for Mechanical Testing of Steel Products, ASTM International, West Conshohocken PA, 2017, Available from: https://www.astm.org/Standards/A370.
[23] Japanese Standards Association, Hot-rolled Carbon Steel Strip for Pipes and Tubes, JSC G, 2005 3132.
[24] Sika, Sika Warp −230 C. Product Data Sheet, 13/06/2006.
[25] Sikadur, Sikadur-330.Product Data Sheet, 21/02/2012.
[26] A.A. Hedayat, Prediction of the force displacement capacity boundary of an unbuckled steel slit damper, J. Constr. Steel Res. 114 (2015) 30–50.
[27] T. Kim, A. Whittaker, V. Bertero, A. Gilani, Steel moment resisting connections reinforced with cover and flange plates, Report SAC/BD-00/27, SAC Joint Venture, 2000.